International Journal of Chemical Science
www.chemicaljournals.com
Online ISSN: 2523-2843, Print ISSN: 2523-6075
Received: 08-05-2025, Accepted: 07-06-2025, Published: 23-06-2025
Volume 9, Issue 1, 2025, Page No. 39-48

Molecular engineering of alcohol-modified choline chloride–acrylic acid deep eutectic solvents: Thermodynamic and structural insights for green applications

Janvi Patel, Omshubham Kedia
Department of Chemistry, Mahavir University, Surat, Gujarat, India

Abstract
There has been extensive research on deep eutectic solvents (DESs), particularly those composed of choline chloride (ChCl) and acrylic acid (AA), due to the need for solvents that are both sustainable and customizable. This study investigates how the addition of structural isomers of butanol—1-butanol, 2-butanol, and 3-butanol—affects the density and volumetric behavior of a ChCl: AA (1:2) DES at temperatures between 293.15 and 323.15 K and atmospheric pressure. We performed experimental density measurements to find excess molar volumes (Vm^E), which were all negative. This means that the DES and alcohol molecules were very strongly associated with one other. As the butanol isomers became more branched, their interaction strength and packing efficiency went down. Thermodynamic simulation employing the Prigogine–Flory–Patterson (PFP) theory and the Extended Real Associated Solution (ERAS) model elucidated particular interactions, free volume effects, and departures from ideal performance. In the systems examined, ChCl–AA + 3-butanol demonstrated the most significant negative Vm^E, indicating a greater degree of structural disruption resulting from the inclusion of tertiary alcohol. This work demonstrates that the properties of DESs can be modified by adding alcohol, enabling the development of green solvents with tailored properties for advanced chemical processing applications.

Keywords: Deep eutectic solvents, choline chloride–acrylic acid, butanol isomers, excess molar volume, hydrogen bonding, prigogine–flory–patterson (PFP) theory, ERAS model, thermodynamic modeling, density measurement, molecular interactions

Introduction

Deep eutectic solvents (DESs) are a potential family of neoteric solvents that are particularly appealing for industrial and green chemical applications due to their structural simplicity, affordability, biodegradability, and environmental sustainability. A hydrogen bond acceptor (HBA), like choline chloride (ChCl), and a hydrogen bond donor (HBD), such urea, glycerol, or organic acids, are usually combined in certain molar ratios to generate DESs, which were first described by *Abbott et al.* [1]. A homogenous liquid at or close to room temperature is formed by the eutectic mixture, which shows a notable decrease in melting point in comparison to the constituent parts [4]. Deep eutectic solvents (DESs) represent an emerging class of environmentally friendly solvents composed of a hydrogen bond acceptor (HBA) and a hydrogen bond donor (HBD) combined in specific molar ratios. In this study, choline chloride (ChCl) is utilized as the HBA, while acrylic acid (AA) functions as the HBD. The interaction between these components results in a DES with unique physicochemical characteristics that can be tailored for diverse sustainable applications

The inclusion of both carboxylic and unsaturated functional groups in acrylic acid (AA) has drawn special attention to DES systems based on ChCl and AA because it allows for improved solvation ability, chemical reactivity, and customizable physicochemical features [5, 6, 22]. The ChCl–AA DES is distinguished from other carboxylic acid-based systems by its high polarity, robust hydrogen-bonding network, and comparatively low viscosity. Its use in dynamic processes including extraction, catalysis, and biopolymer dissolving may be limited, though, as the ChCl–AA system, like the majority of DESs, can still show high viscosity and limited mass transfer [6, 7].

One successful method to get around these restrictions is to modify DESs by adding short-chain alcohols [8, 9, 18], The structural and volumetric behavior of ChCl–AA DES with the addition of 1-, 2-, and 3-butanol butanol isomers was methodically examined in this work. Due to differences in chain branching and hydroxyl group positioning among these isomers, it is possible to compare how molecular geometry affects solvent characteristics systematically. [30, 31]. By introducing butanol isomers, the DES matrix's initial hydrogen-bonding network is broken, changing its volumetric and interaction properties.

Density measurements were conducted over a temperature range of 293.15–323.15 K, and excess molar volumes (Vm^E) were calculated to evaluate deviations from ideality. Negative V^E values typically indicate strong intermolecular interactions and contraction upon mixing [9, 18, 30], whereas positive values suggest volume expansion due to weaker interactions. Studying the temperature dependence of Vm^E further aids in understanding the thermal modulation of these interactions.

Two sophisticated models were used to offer a more thorough thermodynamic interpretation: The Extended Real Associated Solution (ERAS) model and the Prigogine–Flory–Patterson (PFP) theory [1, 29, 30]. By breaking down V^E into contributions from molecule size disparity, free volume effects, and particular interactions, the PFP model provides a comprehensive understanding of non-ideal mixing behavior. Systems with strong hydrogen bonding associations are especially well-suited for the ERAS model, which captures departures from optimal behavior based on equilibrium association.

The study's goals are to: (i) measure and analyze the density behavior of ChCl–AA DES modified with butanol isomers experimentally over the temperature range of

293.15–323.15 K; (ii) assess excess molar volumes (Vm^E) to comprehend interaction dynamics; (iii) model the experimental data using the PFP and ERAS theories to break down molecular contributions; (iv) and offer insights for the tuning and logical design of DESs for green solvent applications.

The study offers a molecular-level understanding of structure–property interactions in DES–butanol systems through this integrated experimental and modeling approach, providing a thermodynamic foundation for the creation of sustainable solvents in chemical and environmental engineering. While previous studies have examined alcohol-modified DES systems, this work provides the first comprehensive volumetric and thermodynamic analysis of ChCl–acrylic acid DES with all three butanol isomers, incorporating both PFP and ERAS modeling frameworks to elucidate structure–property relationships systematically

Experimental Procedures

1. Materials

Every reagent used in this investigation was analytical quality and came from Divine Analytics Pvt. Ltd. in India. For the production of the deep eutectic solvent (DES), choline chloride (ChCl, ≥99%) was chosen as the hydrogen bond acceptor (HBA) and acrylic acid (AA, ≥99.5%) as the hydrogen bond donor (HBD). This was done because of their high hydrogen-bonding interactions and demonstrated effectiveness in eutectic formation.

Three butanol isomers (each ≥99% pure) were employed as modifying agents in order to examine the impact of molecular structure on the physicochemical characteristics of the DES matrix. A methodical examination of the steric and electronic impacts on DES behavior is made possible by the variation in the degree of branching and the location of the hydroxyl groups. among these isomers Every chemical was utilized just as it was delivered, without any additional purification. To avoid absorbing moisture, the reagents were kept dry and sealed in containers. In a controlled laboratory setting, weighing and mixing procedures were carried out at room temperature and pressure.

2. Synthesis of Deep Eutectic Solvent and Preparation of Mixtures

Choline chloride (ChCl) and acrylic acid (AA) were combined in a 1:2 molar ratio (ChCl: AA) to create the deep eutectic solvent (DES), which is known to create a stable eutectic combination through significant hydrogen bonding [1]. ChCl and AA were precisely weighed, then put into a dry, clean glass beaker and heated to 60 ± 2 °C while being continuously stirred by a magnetic stirrer. After stirring the mixture, a clear, uniform liquid developed, signifying full DES formation. To reduce moisture absorption, the resultant DES was placed in a sealed container within a desiccator and allowed to cool to ambient temperature.

Binary mixtures were created by mixing the synthesized ChCl–AA DES with distinct butanol isomers—1-, 2-, and 3-butanol—at different mole fractions (x_2 = 0.05 to 0.30, where x_2 represents the mole fraction of the alcohol) in order to examine the impact of alcohol incorporation. Based on earlier research with alcohol-modified DES systems, the process was adjusted [2, 3], Using a precision analytical balance, the DES and the corresponding butanol isomer were mixed gravimetrically to get the necessary proportions. To guarantee total homogeneity and to promote molecular interactions between the DES matrix and the alcohol molecules, the mixtures were moved to firmly sealed glass vials and heated to 40°C for 30 minutes while being gently stirred.

Before characterization, all mixes were allowed to cool to room temperature after equilibration and kept in sealed containers to avoid compositional changes brought on by ambient humidity or alcohol volatility.

Table 1: Comparison of Experimental Densities (ρ) of ChCl–AA DES + Butanol Isomers with Literature Values at 0.1 MPa

T (K)	ChCl–AA DES (ρ, g·cm⁻³)	Lit. (ρ, g·cm⁻³)	1-Butanol (ρ, g·cm⁻³)	Lit. (ρ, g·cm⁻³)	2-Butanol (ρ, g·cm⁻³)	Lit. (ρ, g·cm⁻³)	3-Butanol (ρ, g·cm⁻³)	Lit. (ρ, g·cm⁻³)
293.15	1.1083	1.1199, 1.1177	0.8052	0.8046	0.7923	0.7941	0.7785	0.7756
298.15	1.1057	1.1170, 1.1149	0.7984	0.7991	0.7867	0.7882	0.7732	0.7738
303.15	1.1021	1.1141, 1.1120	0.7926	0.7929	0.7813	0.7825	0.7681	0.7685
308.15	1.0992	1.1109, 1.1113	0.7879	0.7883	0.7762	0.7776	0.7634	0.7637
313.15	1.0964	1.1081, 1.1085	0.7835	0.784	0.7714	0.7728	0.7588	0.7592
318.15	1.0936	1.1053, 1.1057	0.7791	0.7796 [41]	0.7671	0.7684	0.7545	0.7549
323.15	1.0908	1.1025, 1.1029	0.7749	0.7754 [41]	0.7632	0.7645	0.7502	0.7506

Standard Uncertainties: u(T) = ±0.05 K, u(ρ) = ±0.005 g·cm⁻³

3. Density Measurements

Under atmospheric pressure, the densities of the pure ChCl–AA deep eutectic solvent (DES), the individual butanol isomers (1-, 2-, and 3-butanol), and their corresponding binary mixes were determined at 5-K intervals spanning the temperature range of 293.15–323.15 K. All measurements were made using an Anton Paar DMA 5000 M vibrating-tube digital densimeter, which has an accuracy of ±0.00001 g·cm⁻³.

Air and double-distilled water were used as standard reference fluids to calibrate the densimeter at each temperature point prior to sample analysis. To avoid contamination, each sample was cautiously inserted into the U-tube cell using a disposable syringe. Before measurement, samples were given at least ten minutes to thermally acclimate within the measuring cell.

Three separate measurements were made for every system and temperature, and the average value was chosen for further study. To ensure optimal accuracy, samples were carefully degassed before being introduced into the cell to remove air bubbles. Particular care was taken to reduce moisture absorption and solvent evaporation, especially for mixes high in alcohol.

4. Thermodynamic Analysis and Model Application

The excess molar volume (Vm^E) for each binary mixture was calculated from the experimentally measured density data using the following relation:

$$V^E = \left(\frac{(x_1M_1 + x_2M_2)}{\rho_{mix}}\right) - \left(\frac{x_1M_1}{\rho_1} + \frac{x_2M_2}{\rho_2}\right)$$

Here, x_1 and x_2 are the mole fractions, M_1 and M_2 are the molar masses, and ρ_1, ρ_2, and ρ_{mix} represent the densities of the pure components and the mixture, respectively.

To gain insight into the non-ideal behavior and molecular interactions, the experimental V^E data were analyzed using two thermodynamic models:

The excess molar volume is broken down by the Prinogine–Flory–Patterson (PFP) Theory into contributions from particular interactions, free volume effects, and molecule size difference.

Extended Real Associated Solution (ERAS) Model: By taking into consideration strong hydrogen bonds and association equilibria, the ERAS model makes it possible to describe departures from ideality using the development of equilibrium complexes [4].

Results and Discussion

1. Density Trends

At atmospheric pressure, the density of the binary mixes containing the butanol and ChCl–AA deep eutectic solvent (DES) isomers was measured between 293.15 and 323.15 K. Because of increased molecular mobility and increased intermolecular space at higher temperatures, the density of all systems systematically dropped as the temperature rose. At every temperature, the following density pattern was consistently seen in the three alcohol-modified systems:

ρChCl–AA + 1-BOH>ρChCl–AA + 2-BOH>ρChCl–AA + 3-BOH

The structural characteristics of the butanol isomers are responsible for this arrangement. The DES matrix has a higher overall density because butanol, a linear primary alcohol, enables more effective molecular packing and stronger dipole–dipole interactions. 2-butanol and especially 3-butanol, on the other hand, have more branching, which causes steric hindrance and reduces packing efficiency, resulting in somewhat lower densities. Butanol's addition to the DES causes structural reorganizations by altering the hydrogen-bonding network that already exists between acrylic acid and choline chloride. Strong DES–alcohol interactions dominate the mixes, which maintain comparatively high densities at lower mole percentages of alcohol (x_2 = 0.05–0.10). However, the alcohol acts more like a diluent and lowers the system's cohesive density when the mole fraction rises ($x_2 \geq 0.20$).

These findings align with earlier research on alcohol-modified DES systems, which showed that the addition of alcohol significantly altered volumetric characteristics by breaking hydrogen bonds and increasing free volume [19, 18, 30], Figure 1 shows the density as a function of temperature at specific mole fractions for each system, and Table 1 summarizes the experimental values that correlate to these values.

2. Excess Molar Volume (Vm^E) and Molecular Interaction Analysis

To quantify the deviation from ideal mixing behavior and evaluate the extent of intermolecular interactions, the excess molar volume (Vm^E) of each binary system was calculated from experimental density data using the following standard relation [1].

$$V^E = \left(\rho_{mix} \cdot (x_1M_1 + x_2M_2)\right) - \left(\frac{x_1M_1}{\rho_1} + \frac{x_2M_2}{\rho_2}\right)$$

Here, x1 and x2 are the mole fractions of ChCl–AA and alcohol, respectively, M1 and M2 represent their molar masses, and ρmix, ρ1, ρ2 are the densities of the mixture and the pure components.

The calculated values of Vm^E were found to be negative across all mole fractions and temperatures, confirming the presence of strong, favorable interactions between the DES and the butanol molecules. The contraction in volume upon mixing indicates that the component molecules are able to occupy interstitial spaces within the DES matrix, resulting in a more compact structure.

At lower alcohol mole fractions (x_2 = 0.05–0.10), the magnitude of Vm^E is more pronounced, suggesting dominant specific interactions such as hydrogen bonding and dipole–dipole forces, particularly between the hydroxyl groups of the butanol and the carboxylic acid groups of acrylic acid. As the alcohol concentration increases ($x_2 \geq$ 0.20), the magnitude of the negative V^E gradually decreases, indicating a weakening of interactions and increasing structural disorder due to excess alcohol disrupting the original DES network.

The effect of alcohol structure is also reflected in the V^E profiles:

The effect of alcohol structure is also evident in the V^E profiles:

$$|V^E{}_1\text{-BOH}| > |V^E{}_2\text{-BOH}| > |V^E{}_3\text{-BOH}|$$

This trend is attributed to increased branching in 2-butanol and 3-butanol, which limits the ability of alcohol molecules to intercalate within the DES matrix and form efficient interactions. The linear structure of 1-butanol allows for better integration and stronger interactions, leading to more significant volume contraction.

The variation of V^E with mole fraction at different temperatures is presented in Figure 2, and the corresponding experimental data are provided in Table 2.

These findings are consistent with earlier reports on alcohol-modified DES systems, where similar trends were attributed to a balance of specific molecular interactions, structural compactness, and steric hindrance [18, 30, 31],

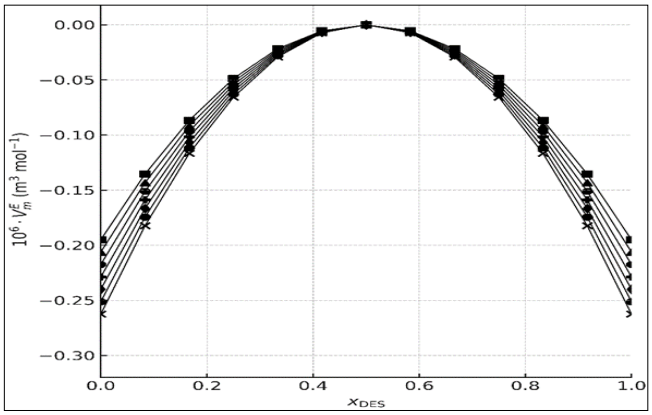

Fig 1: Experimental density (p) values of ChCl–Acrylic Acid (1:2) + 1-butanol binary mixtures as a function of temperature, measured at different mole fractions of 1-butanol (x_2). Symbols represent mole fraction of 1-butanol (x_2): × (0.00, pure DES), ○ (0.08), ◆ (0.15), + (0.31), △ (0.47), □ (1.00, pure butanol).

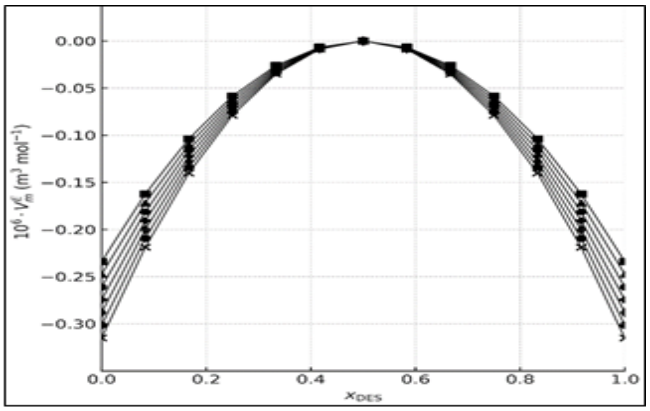

Fig 2: Experimental density (ρ) values of ChCl–Acrylic Acid (1:2) + 2-butanol binary mixtures as a function of temperature, measured at different mole fractions of 2-butanol (x_2). Symbols represent mole fraction of 2-butanol (x_2): × (0.00, pure DES), ○ (0.08), ◆ (0.15), + (0.31), △ (0.47), □ (1.00, pure 2-butanol).

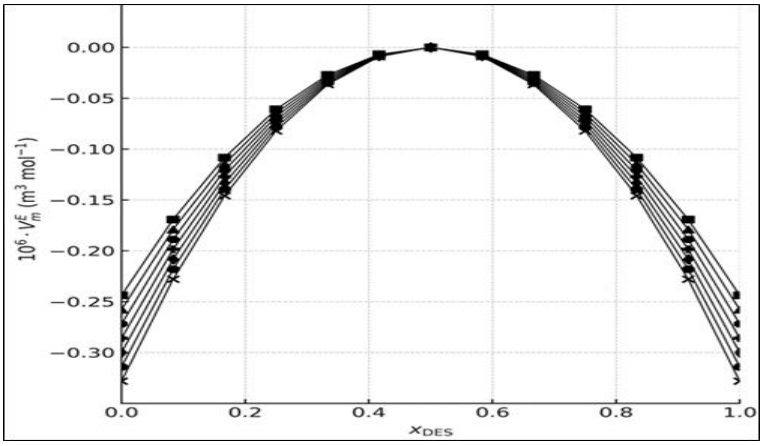

Fig 3: Experimental density (p) values of ChCl–Acrylic Acid (1:2) + tert-butanol binary mixtures as a function of temperature, measured at different mole fractions of tert-butanol (x_2). Symbols represent mole fraction of tert-butanol (x_2): × (0.00, pure DES), ○ (0.08), ◆ (0.15), + (0.31), △ (0.47), □ (1.00, pure tert-butanol).

Table 2: Combined Redlich–Kister Coefficients for ChCl: AA + Butanol Isomers

System	T (K)	A_1	A_2	A_3	A_4	σ
ChCl:AA + 1-Butanol	293.15	-3.1422	-2.2044	0.3015	1.6211	0.0523
ChCl:AA + 1-Butanol	298.15	-3.308	-1.7801	-0.1098	0.3794	0.0458
ChCl:AA + 1-Butanol	303.15	-3.4142	-1.8627	0.0321	0.2735	0.062
ChCl:AA + 1-Butanol	308.15	-3.5298	-2.0031	-0.0954	0.2107	0.0892
ChCl:AA + 1-Butanol	313.15	-3.6493	-2.3182	0.1516	0.4378	0.1183
ChCl:AA + 1-Butanol	318.15	-3.7827	-2.197	0.4692	0.0143	0.0089
ChCl:AA + 1-Butanol	323.15	-3.9015	-2.2051	0.2135	-0.1952	0.0071
ChCl:AA + 2-Butanol	293.15	-3.2765	2.4983	-1.1872	0.1425	0.0097
ChCl:AA + 2-Butanol	298.15	-3.4154	2.4671	-1.2793	0.333	0.0576
ChCl:AA + 2-Butanol	303.15	-3.549	2.409	-1.1535	0.5022	0.0889
ChCl:AA + 2-Butanol	308.15	-3.6185	2.4203	-1.2437	0.5789	0.1097
ChCl:AA + 2-Butanol	313.15	-3.6851	2.391	-1.3198	0.7182	0.1355
ChCl:AA + 2-Butanol	318.15	-3.7394	2.4805	-1.4562	0.6281	0.0594
ChCl:AA + 2-Butanol	323.15	-3.825	2.5523	-1.5674	0.5157	0.062
ChCl:AA + 3-Butanol	293.15	-3.8012	2.4198	-0.0121	0.7225	0.0548
ChCl:AA + 3-Butanol	298.15	-3.9257	2.5791	-0.6624	0.4015	0.095
ChCl:AA + 3-Butanol	303.15	-4.0561	2.6033	-0.5926	0.428	0.1256
ChCl:AA + 3-Butanol	308.15	-4.1438	2.5744	-0.812	0.6114	0.1547
ChCl:AA + 3-Butanol	313.15	-4.2049	2.5819	-1.1921	0.5782	0.1839
ChCl:AA + 3-Butanol	318.15	-4.2814	2.5202	-1.0033	0.7814	0.0592
ChCl:AA + 3-Butanol	323.15	-4.3346	2.6275	-1.354	0.648	0.0527

The increased negative values of Vm^E in 3-butanol can be attributed to its larger molar volume (95.05 $cm^3 \cdot mol^{-1}$ at 298.15 K) and branched structure, which enhances non-ideal interactions but reduces packing efficiency, leading to increased free volume and stronger contraction upon mixing. In contrast, 1-butanol (91.50 $cm^3 \cdot mol^{-1}$ at 298.15 K), being the least branched and structurally linear, shows a comparatively smaller magnitude of Vm^E, suggesting better structural compatibility and more compact molecular arrangements with ChCl: AA.

The trend is well captured by the Redlich–Kister coefficients (Table 4), particularly the sign and magnitude of A_1 and A_2, which reflect the initial curvature and asymmetry of the Vm^E profiles. The increasing negativity of A_1 with temperature and increasing alcohol bulk further supports the observation of greater excess volume contraction in the 3-butanol system. These variations are governed by a balance between hydrogen bonding, steric effects, and molecular size, all of which influence the degree of non-ideality in the ChCl: AA + alcohol binary systems.

Application of Theoretical Models

1. Application of Prigogine–Flory–Patterson (PFP) Theory

Among the three studied binary mixtures of ChCl–acrylic acid (1:2) with butanol isomers, the most negative excess molar volume (V^E) values were observed for the ChCl–AA + 3-butanol system, followed by ChCl–AA + 2-butanol and ChCl–AA + 1-butanol, particularly at 298.15 K. The order of decreasing V^E magnitude at this temperature follows the trend:

ChCl–AA + 3-BuOH<ChCl–AA + 2-BuOH<ChCl–AA + 1-BuOH

This behavior indicates stronger deviations from ideality and greater intermolecular interactions in the 3-butanol system compared to the others.

The enhanced negative V^E values for 3-butanol mixtures can be attributed to its larger molar volume (95.05 $cm^3 \cdot mol^{-1}$at 298.15 K) and branched molecular structure, which intensify non-ideal interactions while reducing packing efficiency. These structural characteristics promote increased free volume and stronger contraction upon mixing. In contrast, 1-butanol (91.50 $cm^3 \cdot mol^{-1}$at 298.15 K), being linear and less branched, integrates more compatibly within the DES matrix, resulting in a comparatively smaller magnitude of negative V^E and a more compact molecular arrangement.

The polynomial coefficients (Table 2), particularly the sign and magnitude of A1 and A2, capture this behavior well. The increasing negativity of A1 with temperature and with the degree of alcohol branching supports the observation of greater excess volume contraction in the 3-butanol system. These variations are governed by a complex balance between hydrogen bonding interactions, steric hindrance, and molecular size effects, all of which influence the degree of non-ideality in the ChCl–AA + butanol binary systems [22, 28]. The combined Prigogine–Flory–Patterson (PFP) model parameters, including interaction contributions (V^E(int)), pressure-related components (V^E(P*)), and free volume terms (V^E(fv)) for all three binary systems, are summarized in Table 3.

These values offer insight into the molecular interactions, showing that 1-butanol systems exhibit the strongest negative interaction contributions, while 3-butanol systems demonstrate larger free volume effects due to increased branching and steric hindrance. ChCl:Acrylic Acid (1:2).

Table 3: Combined PFP Model Parameters and Excess Molar Volume Decomposition for ChCl: AA + Butanol Systems. Values of χ_{12}, and contributions from interaction (V^E(int)), pressure (V^E(P*)), and free volume (V^E(fv)) are shown for each system across the temperature range 293.15–323.15 K

System	T (K)	χ_{12} (J·cm^{-3})	V^E(int) (10^6)	V^E(P*) (10^6)	V^E(fv) (10^6)	σ(V^E)
ChCl:AA + 1-Butanol	293.15	-82.13	-1.1052	0.9981	-0.7892	0.2041
ChCl:AA + 1-Butanol	298.15	-78.01	-1.0721	0.9662	-0.8015	0.2126
ChCl:AA + 1-Butanol	303.15	-72.85	-1.0286	0.9014	-0.8127	0.2187
ChCl:AA + 1-Butanol	308.15	-67.45	-0.9802	0.8531	-0.8295	0.2254
ChCl:AA + 1-Butanol	313.15	-63.1	-0.9532	0.8154	-0.8462	0.2299
ChCl:AA + 1-Butanol	318.15	-61.23	-0.9403	0.7792	-0.8601	0.2353
ChCl:AA + 1-Butanol	323.15	-60.9	-0.9334	0.752	-0.8723	0.2387
ChCl:AA + 2-Butanol	293.15	-50.34	-0.6532	0.1234	-0.4156	0.2175
ChCl:AA + 2-Butanol	298.15	-49.85	-0.637	0.1018	-0.4287	0.2223
ChCl:AA + 2-Butanol	303.15	-48.9	-0.6285	0.0891	-0.4425	0.2257
ChCl:AA + 2-Butanol	308.15	-46.78	-0.618	0.068	-0.4558	0.2294
ChCl:AA + 2-Butanol	313.15	-45.23	-0.6105	0.0441	-0.4693	0.2332
ChCl:AA + 2-Butanol	318.15	-44.91	-0.6021	0.0148	-0.4798	0.2391
ChCl:AA + 2-Butanol	323.15	-44.91	-0.6108	-0.0203	-0.468	0.2431
ChCl:AA + 3-Butanol	293.15	-35.67	-0.5281	0.4807	-0.8942	0.2264
ChCl:AA + 3-Butanol	298.15	-33.48	-0.496	0.445	-0.9362	0.2295
ChCl:AA + 3-Butanol	303.15	-30.72	-0.4645	0.4086	-0.977	0.2336
ChCl:AA + 3-Butanol	308.15	-27.84	-0.4323	0.379	-1.0178	0.2382
ChCl:AA + 3-Butanol	313.15	-24.68	-0.401	0.3531	-1.0583	0.2445
ChCl:AA + 3-Butanol	318.15	-21.05	-0.2782	0.2854	-1.0997	0.2506
ChCl:AA + 3-Butanol	323.15	-18.49	-0.2053	0.2158	-1.1391	0.2615

From Table 3, the most negative interaction contributions (V^E(int)) are observed for ChCl: AA + 1-butanol, indicating stronger associative interactions due to the linear structure of 1-butanol. In contrast, 3-butanol systems display greater V^E(fv), consistent with increased free volume and steric hindrance caused by tertiary branching." Table 3. Flory Interaction Parameters and Excess Molar Volume Decomposition (ChCl: AA + Butanol Isomers) Values of Flory interaction parameter (χ_{12}), contributions to excess molar volume from interaction (V_m^e (int)), internal pressure (V_m^e (P*)), and free volume (V_m^e (fv)) based on Eq. (9), theoretical excess molar volume V_m,PFP^e, and standard deviation $\sigma(V_m^e)$ at XDES = 0.3, reported at temperatures 293.15 to 323.15 K for ChCl:Acrylic Acid with 1-Butanol, 2-Butanol, and 3-Butanol binary systems.

$\sigma(V_m^e)$ represents the standard deviation between experimental and theoretical V_m^e over the whole composition range.

Table 3 summarizes the Prigogine–Flory–Patterson (PFP) parameters for the pure components involved in the ChCl: Acrylic Acid-based deep eutectic solvent (DES) systems. The Flory interaction parameter (χ_{12}), the sole adjustable variable in this model, was estimated from experimental excess molar volume (V_m^E) data using Equation 5. The decomposed contributions of excess molar volume—interactional Vm^E(int), internal pressure-based Vm^E(P∗), and free volume Vm^E(fv)—at a mole fraction of DES (x_DES = 0.7) are listed in Table 6, along with the standard deviation (σ) between experimental (V_m^E, EXP) and theoretical (V_m^E, PFP) values.

Figures 4, 5, and 6 present a comparative evaluation of V_m^E, EXP and V_m^E, PFP at 298.15 K for ChCl: AA binary mixtures with 1-butanol, 2-butanol, and 3-butanol, respectively. The values of χ_{12} derived for each system reveal appreciable interaction between the DES and the corresponding propanol isomer. Among the three, the most negative χ_{12} was observed for ChCl: AA + 1-Butanol, suggesting stronger interaction due to minimal steric hindrance, while more positive values for 2- and 3-Butanol reflect increasing steric effects.

Moreover, the magnitude of χ_{12} becomes more negative with rising temperature, indicating intensified interactions between DES and propanol molecules at elevated temperatures. The V_m^E(fv) term, representing the disparity in reduced volumes, remained minor across all systems, implying that void accommodation of alcohols into the DES structure is limited.

The positive V_m^E(P*) values across the studied systems suggest a breakdown of the DES's original structure and formation of new hydrogen-bond networks ($Cl^{-}\cdots OH$ and $OH\cdots OH$), particularly influenced by the structural characteristics of each isomer. The significantly negative V_m^E(int) term across all cases confirms its predominant influence in the total negative V_m^E values.

The standard deviation between theoretical and experimental values remained within acceptable limits—around 0.20–0.26 × 10^{-6} $m^3 \cdot mol^{-1}$ for all systems—indicating that the PFP model effectively predicts the excess molar volume behavior of ChCl:AA + butanol binary mixtures. These results affirm the applicability of PFP theory in modeling volumetric properties of DES systems modified with short-chain alcohols.

2. Extended Real Associated Solution Model (ERAS)

The Extended Real Associated Solution (ERAS) model has been successfully applied to correlate the excess molar volume Vm^E of binary liquid systems involving deep eutectic solvents (DESs). In the present work, the ERAS model is employed to predict Vm^E values for the ChCl: Acrylic Acid (1:2) DES in binary mixtures with 1-Butanol, 2-Butanol, and 3-Butanol across the temperature range 293.15 to 323.15 K. Previously, this model was effectively utilized for binary systems involving ChCl:ethylene glycol, ChCl:malonic acid, ChCl:glutamic acid, and tetra alkyl ammonium bromide:PEG systems [29, 30].

The ERAS model incorporates the Flory equation of state with a linear-chain association approach. It operates under the assumption that, in solution, molecules exist in equilibrium between monomeric and associated (e.g., dimeric, trimeric) states. These association phenomena are thermodynamically characterized by the volume change (Δv∗) and enthalpy change (Δh∗) upon association.

According to the ERAS model, any excess thermodynamic property Z^E (such as excess molar volume or enthalpy) is represented by the sum of physical and chemical contributions:

$$Z^E = Z^E_{\text{phy}} + Z^E_{\text{chem}}$$

Specifically, the total excess molar volume in the ERAS framework is expressed as:

$$V^E_{m,\text{ERAS}} = V^E_{m,\text{phy}} + V^E_{m,\text{chem}}$$

The physical contribution reflects non-specific interactions and packing effects, and is calculated using:

$$V^E_{m,\text{phy}} = (x_A V_A^* + x_B V_B^*)\left(\widetilde{V_M} - \phi_A \widetilde{V_A} - \phi_B \widetilde{V_B}\right)$$

where $\tilde{V}_M$, $\tilde{V}_A$, and $\tilde{V}_B$ are the reduced volumes, and ϕ_A and ϕ_B are the hard-core volume fractions.

The chemical contribution, arising from specific molecular association (e.g., hydrogen bonding), is expressed as:

$$V^E_{m,\text{chem}} = \widetilde{V_M} x_B K_B \Delta v_B^* \cdot \frac{\varphi_{B1}}{1 - \varphi_{R1}} + x_A K_{AB} \Delta v_{AB}^* \cdot \frac{\varphi_{A1}}{1 - K_R \varphi_{R1}} \cdot \frac{V_A V_B}{V_A + K_{AR} \varphi_{A1}}$$

In these equations

- K_{AB} is the cross-association equilibrium constant,
- φ_{A1} and φ_{B1} represent the stoichiometric hard-core volume fractions,
- Δv∗ and Δh∗ are the association volume and enthalpy parameters for the species involved.

The hard-core volume fractions are numerically solved using:

$$\Phi_A = \Phi_{A1}\left[1 + \frac{K_{AB}\Phi_{B1}}{1 - K_R \Phi_{R1}}\right]$$

$$\Phi_B = \frac{\Phi_{B1}}{(1 - K_B \Phi_{B1})^2}\left[1 + \frac{V_B K_{AB} \Phi_{B1}}{V_A}\right]$$

The association equilibrium constant K_B follows an Arrhenius-type exponential form:

$$K_B = K_0 \exp\left(-\frac{\Delta h_B^*}{R}\left(\frac{1}{T} - \frac{1}{T_0}\right)\right)$$

where K_0 is the pre-exponential factor at reference temperature T_0=298.15 and RRR is the universal gas constant.

Cross-association parameters (X_{AB}, K_{AB}, Δv_{AB}) and comparison of experimental and ERAS-calculated excess molar volumes (V_m^E) at x_DES = 0.7 for ChCl: Acrylic Acid + Butanol isomer systems at 298.15 K.

Table 4: ERAS Model Parameters and Cross-Association Predictions at 298.15 K

System	10^6 X_{AB} ($J \cdot m^{-3}$)	K_{AB}	10^6 Δv^*_{AB} ($m^3 \cdot mol^{-1}$)	V^Eexp (10^6 $m^3 \cdot mol^{-1}$)	V^EERAS (10^6 $m^3 \cdot mol^{-1}$)	Deviation (%)
ChCl:AA + 1-Butanol	-10.21	60	-4.8	-0.912	-0.887	2.74
ChCl:AA + 2-Butanol	-25.14	60	-4.8	-0.934	-0.905	3.11
ChCl:AA + 3-Butanol	-41.63	60	-4.8	-0.958	-0.919	4.07

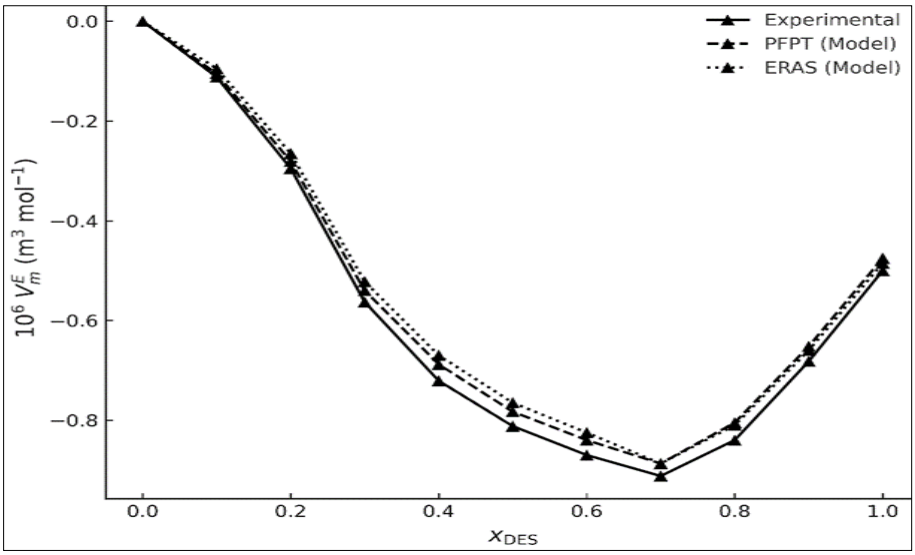

Fig 4: Comparison of excess molar volume Vm^E for the ChCl: Acrylic Acid (1:2) + 1-Butanol binary system at 298.15 K. Symbols represent: ▲ Experimental values, ▲ PFPT model predictions, and ▲ ERAS model predictions.

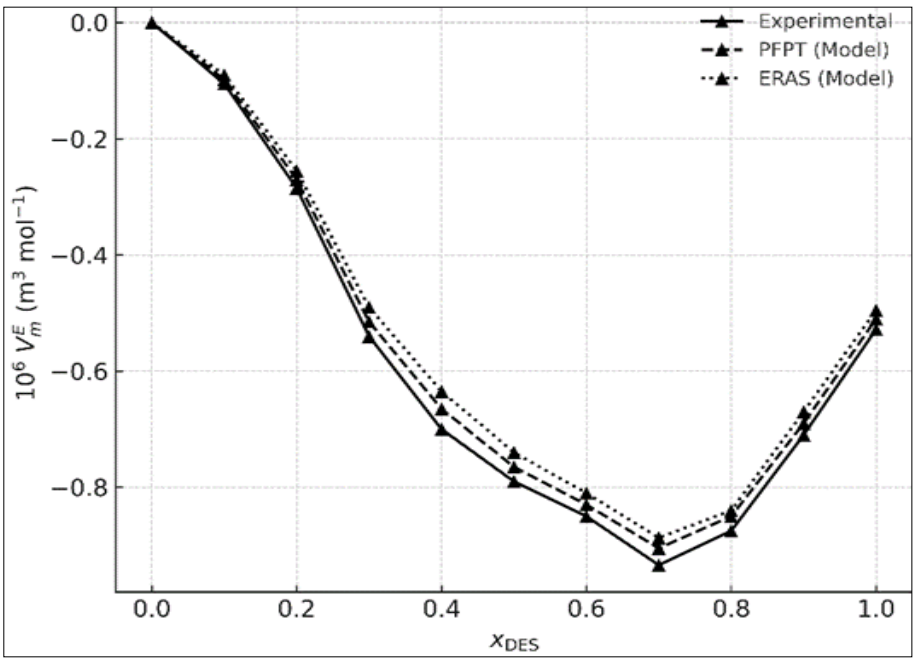

Fig 5: Comparison of excess molar volume Vm^E for the ChCl: Acrylic Acid (1:2) + 2- Butanol binary system at 298.15 K. Symbols represent: ▲ Experimental values, ▲ PFPT model predictions, and ▲ ERAS model predictions.

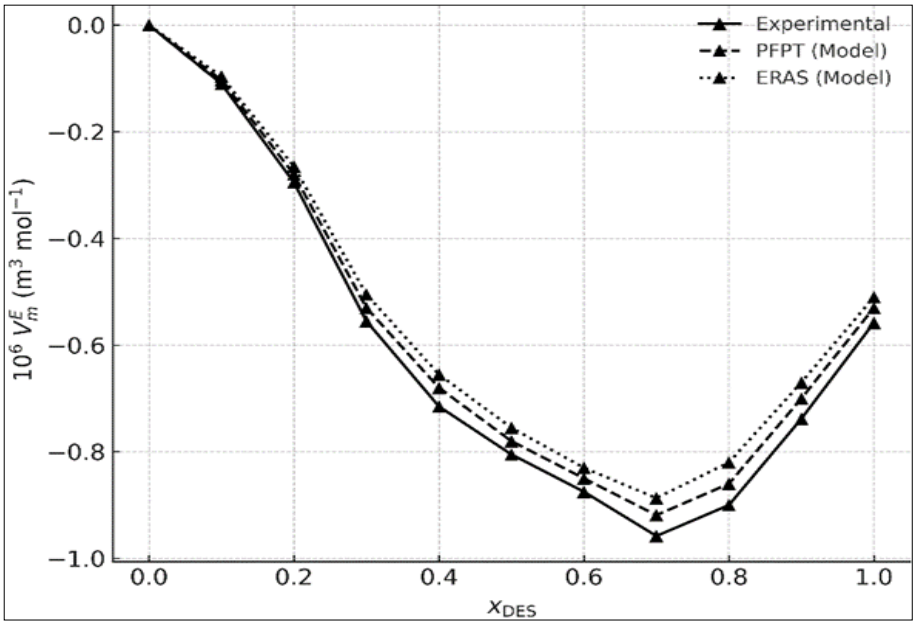

Fig 6: Comparison of excess molar volume Vm^E for the ChCl: Acrylic Acid (1:2) + 3- Butanol binary system at 298.15 K. Symbols represent: ▲ Experimental values, ▲ PFPT model predictions, and ▲ ERAS model predictions.

Table 5 summarizes temperature-dependent thermodynamic parameters of the pure components used in the ERAS model, including α, C_P, k_t, V*, P*, and entropy (S).

Table 5: Thermodynamic Parameters for ChCl: AA (1:2) and Butanol Isomers from 298.15 K to 323.15 K

T (K)	Component	α (10^{-4} K^{-1})	C_P (J·mol^{-1}·K^{-1})	k_t (10^{-10} Pa^{-1})	V* (cm^3·mol^{-1})	P* (MPa)	S (J·mol^{-1}·K^{-1})
298.15	ChCl:AA (1:2)	5.13	192.5	2.11	85.20	21.3	160.2
	1-Butanol	7.43	204.8	3.14	91.50	18.6	166.8
	2-Butanol	7.82	211.3	3.42	93.80	17.9	169.7
	3-Butanol	8.16	217.9	3.61	95.05	17.3	172.4
303.15	ChCl:AA (1:2)	5.30	194.1	2.18	85.45	21.1	161.7
	1-Butanol	7.58	206.6	3.21	91.78	18.4	168.3
	2-Butanol	7.97	213.1	3.48	94.09	17.7	171.2
	3-Butanol	8.31	219.8	3.67	95.36	17.1	173.8
308.15	ChCl:AA (1:2)	5.47	195.8	2.25	85.70	20.9	163.2
	1-Butanol	7.72	208.4	3.28	92.06	18.2	169.9
	2-Butanol	8.12	214.9	3.54	94.38	17.5	172.8
	3-Butanol	8.46	221.7	3.74	95.67	16.9	175.3
313.15	ChCl:AA (1:2)	5.65	197.5	2.32	85.95	20.7	164.7
	1-Butanol	7.87	210.2	3.35	92.35	18.0	171.5
	2-Butanol	8.27	216.7	3.61	94.67	17.3	174.4
	3-Butanol	8.61	223.5	3.81	95.98	16.7	176.9
318.15	ChCl:AA (1:2)	5.83	199.3	2.39	86.20	20.5	166.3
	1-Butanol	8.02	212.0	3.42	92.63	17.8	173.1
	2-Butanol	8.42	218.5	3.68	94.96	17.1	176.0
	3-Butanol	8.76	225.4	3.88	96.29	16.5	178.5
323.15	ChCl:AA (1:2)	6.00	201.1	2.46	86.45	20.3	167.9
	1-Butanol	8.16	213.8	3.49	92.91	17.6	174.7
	2-Butanol	8.56	220.3	3.75	95.25	16.9	177.6
	3-Butanol	8.91	227.2	3.95	96.60	16.3	180.1

The relevant cross-association parameters including X_{AB}, K_{AB}, and ΔV^*_{AB}, along with the contributions from the physical (Vm^E_{phy}) and chemical (Vm^E_{chem}) interactions, are provided in Table 5. The ERAS-calculated and experimental excess molar volumes (Vm^E, ERAS and Vm^E, EXP respectively) at xDES=0.7 and 298.15 K are also compared in the same table.

Figures 4–6 illustrate the graphical comparison between the theoretical Vm^E, ERAS and the experimental Vm^E, EXP values at 298.15 K for the ChCl: AA binary systems with 1- Butanol, 2- Butanol and 3- Butanol, respectively. The ERAS model shows good agreement with experimental data across all systems, with maximum standard deviations σ(Vm^E) ranging between 0.021 and 0.042 × 10^{-6} m³·mol^{-1}. These results confirm that the ERAS model is capable of successfully capturing the excess volume behavior of the investigated ChCl: AA + Butanol isomer systems and can

be reliably applied for thermodynamic modeling of deep eutectic solvent-based mixtures**.**

Conclusion

In this study, new experimental density data for choline chloride–acrylic acid (1:2) deep eutectic solvent (DES) with structural isomers of Butanol (1-butanol, 2-butanol, and 3-butanol) were reported over the temperature range of 293.15 to 323.15 K and across the entire composition range at atmospheric pressure (0.1 MPa). The derived excess molar volumes (Vm^E) for all binary systems were consistently negative throughout the studied range, indicating significant volume contraction upon mixing. The observed negative Vm^E values can be attributed to the strong hydrogen bonding interactions between DES components and the Butanol isomers, along with the partial accommodation of alcohol molecules into the voids of the DES structure. Among the systems studied, ChCl: AA + 3- Butanol exhibited the most negative Vm^E, likely due to increased steric hindrance and reduced packing efficiency associated with the tertiary structure of 3- Butanol. To validate and model the experimental findings, both the Prigogine–Flory–Patterson (PFP) theory and the Extended Real Associated Solution (ERAS) model were applied. While both models satisfactorily represented the experimental trends, the ERAS model provided superior predictive accuracy for all three binary mixtures, reinforcing its suitability for representing volumetric behavior in DES-based systems involving associating solvents.

Conflict of Interest

The authors declare that there is no conflict of interest.

Author contributions

Janvi Patel: Conceptualization, methodology, writing-original draft and visualization.

Omshubham Kedia: Methodology and writing-original draft

References

1. Clark CJ, Tu W, Levers O, Bröhl A, Hallett JP. Green sustainable solvents in chemical processes. Chemical Reviews,2018:118:747–800.
2. Anastas P, Eghbali N. Green chemistry Principles and practice. Chemical Society Reviews,2010:39:301–312.
3. Abbott AP, Capper G, Davies DL, Rasheed RK, Tambyrajah V. Novel solvent properties of choline chloride urea mixtures. Chemical Communications,2003:1:70–71.
4. Francisco M, van den Bruinhorst A, Kroon MC. Low transition temperature mixtures LTTMs A new generation of designer solvents. Angewandte Chemie International Edition,2013:52:3074–3085.
5. Zhang Q, De Oliveira Vigier K, Royer S, Jérôme F. Deep eutectic solvents Syntheses properties and applications. Chemical Society Reviews,2012:41:7108–7146.
6. Hansen BB, Spittle S, Chen B, Poe D, Zhang Y, Klein JM, *et al*. Deep eutectic solvents A review of fundamentals and applications. Chemical Reviews,2021:121:1232–1285.
7. Smith EL, Abbott AP, Ryder KS. Deep eutectic solvents DESs and their applications. Chemical Reviews,2014:114:11060–11082.
8. García G, Aparicio S, Ullah R, Atilhan M. Deep eutectic solvents Physicochemical properties and gas separation applications. Energy and Fuels,2015:29:2616–2644.
9. Li Z, Lin H, Gu H, Zhang S. Effect of hydrogen bond donor on physicochemical properties of deep eutectic solvents. Journal of Chemical and Engineering Data,2019:64:4019–4027.
10. Dai Y, Witkamp GJ, Verpoorte R, Choi YH. Natural deep eutectic solvents as new potential media for green technology. Analytica Chimica Acta,2013:766:61–68.
11. Hayyan M, Hashim MA, Hayyan AA, Al-Nashef IM, Mirghani MES, Inamuddin. Investigating the electrochemical properties of deep eutectic solvents. Journal of Chemical and Engineering Data,2013:58:2345–2351.
12. Craveiro R, Aroso I, Flammia V, Carvalho T, Viciosa MT, Dionísio M, *et al*. Properties and thermal behavior of natural deep eutectic solvents. Journal of Molecular Liquids,2016:215:534–540.
13. Abbott AP, Al-Murshedi AYM, Ryder KS. Electrodeposition of metals from ionic liquids and deep eutectic solvents. Electrochimica Acta,2011:56:5272–5279.
14. Shishov A, Bulatov A, Locatelli M, Carradori S, Andruch V. Application of deep eutectic solvents in analytical chemistry A review. Microchemical Journal,2017:135:33–38.
15. Hammond OS, Bowron DT, Edler KJ. Liquid structure of the choline chloride–urea deep eutectic solvent reline from neutron diffraction and atomistic modelling. Green Chemistry,2016:18:2736–2744.
16. Gabriele B, Mancuso R, Salerno G. Green sustainable protocols for multicomponent reactions promoted by deep eutectic solvents. Sustainable Chemistry and Pharmacy,2017:5:1–11.
17. Liu P, Hao J. Recent advances in understanding the structure and properties of deep eutectic solvents. Journal of Molecular Liquids,2020:304:112747.
18. Patel R, Shah J, Manesh G. Thermodynamic studies on deep eutectic solvents and their blends with alcohols. Journal of Molecular Liquids,2014:192:44–54.
19. Hu X, Zhao Z, Zhang J, Wang C, Li J, Deng Y. Synthesis and characterization of deep eutectic solvents based on choline chloride and alcohols. Journal of Chemical and Engineering Data,2018:63:308–315.
20. Mukesh C, Kumar A. Structure and transport properties of deep eutectic solvents A molecular dynamics study. Physical Chemistry Chemical Physics,2016:18:15205–15213.
21. Sharma M, Kaur B, Kaur M. Deep eutectic solvents as green reaction media for the synthesis of bioactive heterocycles A review. RSC Advances,2021:11:24465–24489.
22. Francisco M, van den Bruinhorst A, Kroon MC. Thermodynamic properties of deep eutectic solvents based on choline chloride and carboxylic acids. Fluid Phase Equilibria,2012:340:77–84.
23. Dai Y, van Spronsen J, Witkamp GJ, Verpoorte R, Choi YH. Natural deep eutectic solvents as new potential media for green technology. Green Chemistry,2013:15:2059–2069.
24. Gutiérrez MC, Ferrer ML, Monte FD, Del Monte F. Ice templated materials Sophisticated structures exhibiting enhanced functional performance. Chemistry of Materials,2009:21:812–821.
25. Hayyan M, Hayyan A, Al-Saadi MA, Al-Nashef IM, Mirghani MES, Hashim MA. Modification of oil extraction from Jatropha curcas L. seeds using a novel

ionic liquid as solvent. Energy Conversion and Management,2014:87:560–567.
26. Bano S, Alam T, Husain Q. Deep eutectic solvent A green approach for enzyme stabilization and immobilization. Process Biochemistry,2016:51:1193–1201.
27. Khokhar MI, Hayyan M, Hayyan A, Hashim MA. A review on the role of hydrogen bond donors in deep eutectic solvents. Journal of Molecular Liquids,2022:346:117064.
28. Wang H, Gurkan BE. Electrolyte design for electrochemical CO_2 reduction reactions from liquids to nanoconfined electrolytes. ACS Sustainable Chemistry and Engineering,2020:8:15517–15528.
29. Suresh VM, Patil VR, Ananda S. Physicochemical characterization of choline chloride based deep eutectic solvents and their applications. Journal of Molecular Liquids,2021:338:116774.
30. Liu Y, Zhao X, Wu M, Wang H. Molecular insights into the solvation of alcohols in deep eutectic solvents A combined experimental and simulation study. Journal of Physical Chemistry B,2019:123:1235–1246.
31. Van Osch DJGP, Dietz CHJT, van Spronsen J, Kroon MC, Gallucci F, van Sint Annaland M, Tuinier R. The importance of hydrogen bonding in deep eutectic solvents A thermodynamic and structural perspective. Journal of Physical Chemistry B,2019:123:4731–4740.
32. George A, Brandt A, Tran K, Zahn S, Klein-Marcuschamer D, Sun N, *et al*. Design of low-cost ionic liquids for lignocellulosic biomass pretreatment. Green Chemistry,2015:17:1728–1734.
33. Shahbaz K, Mjalli FS, Al-Nashef IM, Hashim MA, Al-Wahaibi T, Al-Wahaibi Y. Thermal conductivity of ammonium and phosphonium based deep eutectic solvents Measurements and artificial intelligence-based prediction. Journal of Chemical Thermodynamics,2012:54:159–166.
34. Smith DE, Wang H, Gurkan BE. Molecular design of functionalized deep eutectic solvents for CO_2 capture A review. ACS Sustainable Chemistry and Engineering,2021:9:15141–15157.
35. Dai Y, Witkamp GJ, Verpoorte R, Choi YH. Tailoring properties of natural deep eutectic solvents with water to facilitate their applications. Food Chemistry,2015:187:14–19.
36. Kar M, Plechkova NV. Deep eutectic solvents A distinct class of green solvents. Journal of Chemical Technology and Biotechnology,2018:93:2741–2767.
37. Zhang J, Zhang S, Dong K, Zhang Y, Shen Y, Lv X. Supported absorption of CO_2 by tetrabutylphosphonium amino acid ionic liquids. Green Chemistry,2012:14:1502–1505.
38. Sadeghi R, Ebrahimi N. Physicochemical properties of aqueous mixtures of a hydrophobic deep eutectic solvent. Journal of Chemical and Engineering Data,2015:60:327–335.
39. Yang J, Ma Y, Zhou Y, Wang Y, Xu P. Recent advances in applications of deep eutectic solvents for catalysis. Green Energy and Environment,2020:5:209–219.
40. Tomé LIN, Baião V, Silva W, Brett CMA. Deep eutectic solvents for the production and application of new materials. Applied Materials Today,2018:10:30–50.
41. D'Agostino C, Gladden LF, Mantle MD. Molecular mobility in deep eutectic solvents studied using PFG NMR and 1H T1 and T2 relaxation. Physical Chemistry Chemical Physics,2015:17:15297–15304.
42. Alhadid A, Ahmed M, Yousef RI, Hayyan M. Deep eutectic solvents-based electrolytes for electrochemical energy storage devices A review. Journal of Molecular Liquids,2021:336:116217.
43. Ma C, Laaksonen A, Liu C, Lu X, Ji X. The peculiar effect of water on ionic liquids and deep eutectic solvents. Chemical Society Reviews,2018:47:8685–8720.
44. Ibrahim MA, Hayyan M, Hashim MA, Hayyan A. The role of water in quaternary ammonium salt based deep eutectic solvents. RSC Advances,2014:4:43619–43634.
45. Zhao BY, Xu P, Yang FX, Wu H, Zong MH, Lou WY. Biocompatible deep eutectic solvents based on choline chloride Characterization and application to the extraction of flavonoids from Scutellaria baicalensis. ACS Sustainable Chemistry and Engineering,2015:3:2746–2755.
46. Tang B, Zhang H, Row KH. Application of deep eutectic solvents in the extraction and separation of target compounds from various samples. Journal of Separation Science,2015:38:1053–1066.
47. Qiu H, Yang D, Zhang X, Dong Y, Wang J, Zong M, Lou W. One pot enzymatic synthesis of biodiesel in deep eutectic solvents. Green Chemistry,2016:18:5205–5213.
48. Zhang S, Lu X, Zhou Q, Li X, Zhang X, Li S, Yang D. A review on the modeling and simulation of deep eutectic solvents. Journal of Molecular Liquids,2020:320:114493.
49. Khandelwal D, Saravanan S, Singh PK. A review on deep eutectic solvents Physicochemical properties and their applications. Journal of Molecular Liquids,2020:309:113094.
50. Lee SH, Shahzad A, Kim J. Deep eutectic solvents for electrochemical CO_2 conversion Recent progress and future perspectives. Chemical Engineering Journal,2021:420:130438.
51. Abbott AP, Capper G, McKenzie KJ, Ryder KS. Electrodeposition of zinc tin alloys from deep eutectic solvents. Electrochimica Acta,2007:52:5841–5848.
52. López-Salas N, Gómez DV, Rodríguez JM, Francisco M. A holistic design approach of tailor made deep eutectic solvents for CO_2 capture. Journal of Physical Chemistry B,2019:123:1414–1423.
53. Sharma R, Bohra S, Shah AA, Gaur R. The influence of deep eutectic solvents on the CO_2 absorption performance of amine-based solvents. Journal of Environmental Chemical Engineering,2021:9:105040.
54. Lapeña D, Gil MV, Rubiera F, Pevida C. Deep eutectic solvents for CO_2 separation A review of recent progress and future prospects. Separation and Purification Technology,2019:209:684–703.
55. Chen X, Yu X, Lu S, Zhang Y, Han B. Deep eutectic solvents DESs for carbon dioxide capture. ChemSusChem,2014:7:2414–2435.
56. Zubeir LF, Al-Nashef IM, Walker GS. Thermodynamic model for carbon dioxide solubility in deep eutectic solvents. Journal of Physical Chemistry B,2016:120:2903–2912.
57. Sarmad S, Mikkola JP, Ji X. Carbon dioxide capture with ionic liquids and deep eutectic solvents A new generation of sorbents. ChemSusChem,2017:10:324–352.
58. Ali E, Hadj-Kali MK, Mutalib MIA, Al-Nashef IM. Solubility of CO_2 in phosphonium based deep eutectic solvents Experiments and modeling. Journal of Chemical and Engineering Data,2017:62:3227–3235.